5. G. Pfeffer, K. Majamaa, D. M. Turnbull, D. Thorburn, P. F. Chinnery, *Cochrane Database Syst. Rev.* **4**, CD004426 (2012).
6. N. J. Lake, M. J. Bird, P. Isohanni, A. Paetau, *J. Neuropathol. Exp. Neurol.* **74**, 482–492 (2015).
7. G. S. Gorman *et al.*, *Ann. Neurol.* **77**, 753–759 (2015).
8. S. Parikh *et al.*, *Genet. Med.* **17**, 689–701 (2015).
9. R. H. Haas *et al.*, *Pediatrics* **120**, 1326–1333 (2007).
10. O. Shalem *et al.*, *Science* **343**, 84–87 (2014).
11. T. Wang, J. J. Wei, D. M. Sabatini, E. S. Lander, *Science* **343**, 80–84 (2014).
12. M. P. King, G. Attardi, *Science* **246**, 500–503 (1989).
13. S. E. Calvo, K. R. Clauser, V. K. Mootha, *Nucleic Acids Res.* **44**, D1251–D1257 (2016).
14. M. Ohh *et al.*, *Nat. Cell Biol.* **2**, 423–427 (2000).
15. C. M. Robinson, M. Ohh, *FEBS Lett.* **588**, 2704–2711 (2014).
16. G. L. Wang, B. H. Jiang, E. A. Rue, G. L. Semenza, *Proc. Natl. Acad. Sci. U.S.A.* **92**, 5510–5514 (1995).
17. A. J. Majmundar, W. J. Wong, M. C. Simon, *Mol. Cell* **40**, 294–309 (2010).
18. M. Ivan *et al.*, *Proc. Natl. Acad. Sci. U.S.A.* **99**, 13459–13464 (2002).
19. O. Iliopoulos, A. P. Levy, C. Jiang, W. G. Kaelin Jr., M. A. Goldberg, *Proc. Natl. Acad. Sci. U.S.A.* **93**, 10595–10599 (1996).
20. P. H. Maxwell *et al.*, *Nature* **399**, 271–275 (1999).
21. D. L. Buckley *et al.*, *J. Am. Chem. Soc.* **134**, 4465–4468 (2012).
22. M. H. Rabinowitz, *J. Med. Chem.* **56**, 9369–9402 (2013).
23. N. S. Chandel *et al.*, *Proc. Natl. Acad. Sci. U.S.A.* **95**, 11715–11720 (1998).
24. Y. L. Chua *et al.*, *J. Biol. Chem.* **285**, 31277–31284 (2010).
25. I. Papandreou, R. A. Cairns, L. Fontana, A. L. Lim, N. C. Denko, *Cell Metab.* **3**, 187–197 (2006).
26. D. Tello *et al.*, *Cell Metab.* **14**, 768–779 (2011).
27. J. W. Kim, I. Tchernyshyov, G. L. Semenza, C. V. Dang, *Cell Metab.* **3**, 177–185 (2006).
28. M. C. Simon, *Cell Metab.* **3**, 150–151 (2006).
29. E. van Rooijen *et al.*, *Blood* **113**, 6449–6460 (2009).
30. B. R. Pinho *et al.*, *Br. J. Pharmacol.* **169**, 1072–1090 (2013).
31. K. D. Stackley, C. C. Beeson, J. J. Rahn, S. S. Chan, *PLOS One* **6**, e25652 (2011).
32. J. M. Harris *et al.*, *Blood* **121**, 2483–2493 (2013).
33. K. Santhakumar *et al.*, *Cancer Res.* **72**, 4017–4027 (2012).
34. R. Chowdhury *et al.*, *ACS Chem. Biol.* **8**, 1488–1496 (2013).
35. S. E. Kruse *et al.*, *Cell Metab.* **7**, 312–320 (2008).
36. I. G. Pawson, *Proc. R. Soc. London Ser. B* **194**, 83–98 (1976).
37. J. Caston, N. Jones, T. Stelz, *Neurobiol. Learn. Mem.* **64**, 195–202 (1995).
38. A. Quintana, S. E. Kruse, R. P. Kapur, E. Sanz, R. D. Palmiter, *Proc. Natl. Acad. Sci. U.S.A.* **107**, 10996–11001 (2010).
39. J. Thompson Legault *et al.*, *Cell Rep.* **13**, 981–989 (2015).
40. R. S. Balaban, S. Nemoto, T. Finkel, *Cell* **120**, 483–495 (2005).

ACKNOWLEDGMENTS

We thank W. Kaelin Jr. and members of the Mootha lab for valuable feedback; R. Sharma, M. Ferrari, A. Rogers, and the MGH animal facility for assistance with experiments; and F. van Eeden for Tg(*phd3::EGFP*) zebrafish. I.H.J. is supported by the Department of Energy Computational Science Graduate Fellowship Program (grant DE-FG02-97ER25308). N.E.S. is supported by the National Institutes of Health (NIH) through a NHGRI Pathway to Independence Award (K99-HG008171) and a postdoctoral fellowship from the Simons Center for the Social Brain at the Massachusetts Institute of Technology. F.Z. is supported by NIH through NIMH (grants 5DP1-MH100706 and 1R01-MH110049) and NIDDK (grant 5R01DK097768-03); a Waterman Award from NSF; the New York Stem Cell, Simons, Paul G. Allen Family, and Vallee Foundations; and B. Metcalfe. F.Z. is a New York Stem Cell Foundation Robertson Investigator. W.G. is supported by NIH grants R01DK090311 and R24OD017870 and is a Pew Scholar in the Biomedical Sciences. This work was supported by a gift from the Marriott Mitochondrial Disorders Research Fund (V.K.M.) and a gift in memory of Daniel Garland (V.K.M.). V.K.M. is an Investigator of the Howard Hughes Medical Institute. V.K.M. is a founder of and paid scientific advisor for Raze Therapeutics. W.G. is a paid consultant for FATE Therapeutics. F.Z. is a founder of and a scientific advisor for Editas Medicine and a scientific advisor for Horizon Discovery. V.K.M., I.H.J., L.Z., and W.M.Z. are listed as inventors on a patent application filed by Massachusetts General Hospital related to technology reported in this paper on the use of hypoxia and the hypoxia response in the treatment of mitochondrial dysfunction. F.Z., O.S., and N.E.S. are listed as inventors on a patent application (PCT/US2013/074800) filed by The Broad Institute/MIT related to the genome-scale CRISPR knockout screening technology used in this study. The CRISPR knockout library is available through a Uniform Biological Materials Transfer Agreement from Addgene. The *Ndufs4* KO mice were a kind gift of R. Palmiter and are available under a materials transfer agreement with the University of Washington, Seattle.

SUPPLEMENTARY MATERIALS

www.sciencemag.org/content/352/6281/54/suppl/DC1
Materials and Methods
Figs. S1 to S10
Tables S1 and S2
References (*41–44*)

14 August 2015; accepted 9 February 2016
Published online 25 February 2016
10.1126/science.aad9642

FLOW CHEMISTRY

On-demand continuous-flow production of pharmaceuticals in a compact, reconfigurable system

Andrea Adamo,[1] Rachel L. Beingessner,[2] Mohsen Behnam,[1]* Jie Chen,[1] Timothy F. Jamison,[2]† Klavs F. Jensen,[1]† Jean-Christophe M. Monbaliu,[1]‡ Allan S. Myerson,[1]† Eve M. Revalor,[1]§ David R. Snead,[2]|| Torsten Stelzer,[1]¶ Nopphon Weeranoppanant,[1] Shin Yee Wong,[1]# Ping Zhang[2]**

Pharmaceutical manufacturing typically uses batch processing at multiple locations. Disadvantages of this approach include long production times and the potential for supply chain disruptions. As a preliminary demonstration of an alternative approach, we report here the continuous-flow synthesis and formulation of active pharmaceutical ingredients in a compact, reconfigurable manufacturing platform. Continuous end-to-end synthesis in the refrigerator-sized [1.0 meter (width) × 0.7 meter (length) × 1.8 meter (height)] system produces sufficient quantities per day to supply hundreds to thousands of oral or topical liquid doses of diphenhydramine hydrochloride, lidocaine hydrochloride, diazepam, and fluoxetine hydrochloride that meet U.S. Pharmacopeia standards. Underlying this flexible plug-and-play approach are substantial enabling advances in continuous-flow synthesis, complex multistep sequence telescoping, reaction engineering equipment, and real-time formulation.

Whereas manufacturing of automobiles, electronics, petrochemicals, polymers, and food use an assembly-line and/or continuous, steady-state strategy, pharmaceutical synthesis remains one of the last industrial processes to apply a noncontinuous or "batch" approach. Moreover, pharmaceutical companies generally assemble the active pharmaceutical ingredient (API) using molecular fragments obtained from different sources, with the final synthesis steps done at the company location. The API is then often mixed with excipients and formulated in the final drug product form at a separate plant. As a result, production of a finished dosage form can require up to a total of 12 months, with large inventories of intermediates at several stages. This enormous space-time demand is one of a myriad of reasons that has led to increased interest in continuous manufacturing of APIs and drug products, as well as in the development of integrated processes that would manufacture the drug product from raw materials in a single end-to-end process (*1*–*5*).

Another major challenge facing the pharmaceutical industry is drug shortages; the U.S. Food and Drug Administration (FDA) has reported well over 200 cases per year during 2011–2014 (*6*). The root causes of these shortages often trace back to factors reflective of the limitations of batchwise manufacturing, such as variations in quality control and supply chain interruption. Moreover, the small number of suppliers for any particular medicine further exacerbates the challenges faced by batchwise manufacturing to respond to sudden changes in demand or need,

[1]Department of Chemical Engineering, Massachusetts Institute of Technology, 77 Massachusetts Avenue, Cambridge, MA 02139, USA. [2]Department of Chemistry, Massachusetts Institute of Technology, 77 Massachusetts Avenue, Cambridge, MA 02139, USA.
*Present address: Nuvera Fuel Cells, 129 Concord Road, Billerica, MA 01821, USA. **†Corresponding author. E-mail: tfj@mit.edu (T.F.J); kfjensen@mit.edu (K.F.J); myerson@mit.edu (A.S.M)** ‡Present address: Department of Chemistry, University of Liège, Quartier Agora, Allée du six Août 13, B-4000 Liège (Sart Tilman), Belgium. §Present address: Department of Chemical and Biomolecular Engineering, Faculty of Medicine, Dentistry and Health Sciences, University of Melbourne, 3010 VIC, Australia. ||Present address: Georgia-Pacific Chemicals, 2883 Miller Road, Decatur, GA 30312, USA. ¶Present address: Department of Pharmaceutical Sciences, University of Puerto Rico, Medical Sciences Campus, San Juan, PR 00936, USA. #Present address: Chemical Engineering and Food Technology Cluster, Singapore Institute of Technology, 10 Dover Drive, Singapore 138683. **Present address: Novartis Institute of Biomedical Research, 250 Massachusetts Avenue, Cambridge, MA 02139, USA.

such as in epidemic or pandemic instances of influenza outbreak.

To address the above issues, we have developed a continuous manufacturing platform that combines both synthesis and final drug product formulation into a single, highly compact unit (Fig. 1). The utilization of continuous flow (*7–9*) within the system enables efficient heat and mass transfer, as well as process intensification (*10*) and automation. Over the past several years, the merits of flow chemistry in streamlining synthesis (*11*) have been successfully demonstrated in the preparation of many individual high-profile APIs (*12*, *13*), including artemisinin (*14*), imatinib (*15*), efavirenz (*16*), nabumetone (*17*), rufinamide (*18*), pregabalin (*19*), and (*E/Z*)-tamoxifen (*20*).

Work with colleagues at the Massachusetts Institute of Technology (MIT) on end-to-end, continuous manufacturing of a single API, aliskiren hemifumarate, in a shipping container–sized unit (*21*) enabled us to identify critical steps in on-demand manufacturing of pharmaceuticals. Specifically, we chose to address challenges in reconfiguration for multiple synthesis of multiple compounds, tight integration of process streams for reduced footprint, innovations in chemical reaction and purification equipment, and compact systems for crystallization and formulation. As a result, the current system is ~1/40 the size and reconfigurable, in order to enable the on-demand synthesis and formulation of not just one, but many drug products. With the necessary regulatory approvals, this proof-of-principle system could enable a gradual phase-in of pharmaceutical production in response to demand. Reproduction of the system would be simpler and less costly to operate than a full batch plant and so could produce pharmaceuticals only needed for small patient populations or to meet humanitarian needs. It could be particularly advantageous for drugs with a short shelf life. Furthermore, the ability to manufacture the active ingredient on demand could reduce formulation complexity relative to tablets needing yearlong stability.

The flexible, plug-and-play refrigerator-sized platform (Fig. 1) [1.0 m (width) × 0.7 m (length) × 1.8 m (height), ~100 kg] is capable of complex multistep synthesis, multiple in-line purifications, postsynthesis work-up and handling, semibatch crystallization, real-time process monitoring, and ultimately formulation of high-purity drug products. To demonstrate its capabilities, we produced, from raw materials, sufficient quantities to supply hundreds to thousands of consumable oral or topical liquid doses per day of four different pharmaceuticals: diphenhydramine hydrochloride (**1**), lidocaine hydrochloride (**2**), diazepam (**3**), and fluoxetine hydrochloride (**4**) (Fig. 2) (*22*). The latter API, fluoxetine hydrochloride (**4**), was synthesized as a racemic mixture, as approved by the FDA. These generic molecules from different drug classes have differing chemical structures and synthesis routes, thus challenging the capabilities and exploring the technical limits of the continuous-flow system. Moreover, they are drugs commonly found in a chief medic's toolkit. Diphenhydramine hydrochloride (**1**), for example, well known by the trade name Benadryl, is an ethanolamine-based antihistamine used to treat the common cold,

Fig. 1. Reconfigurable system for continuous production and formulation of APIs. (**A**) Labeled photograph of the stack of upstream synthesis modules. (**B**) Labeled photograph of the downstream purification and formulation modules. (**C**) Close-up examples of upstream units; PFA tube flow reactors in an aluminum shell for heating (left) and membrane surface tension–based separation units (right). (**D**) Images of some of the main components in the downstream unit including the (a) buffer tank, (b) precipitation tank, (c) filtration unit, (d) crystallization unit, (e) filtration unit, (f) formulation tank, (g) solution holding tank, and (h) formulated API. Details are in the supplementary text.

lessen symptoms of allergies, and act as a mild sleep aid. Lidocaine hydrochloride (**2**), alternatively, is a common local anesthetic and class-1b antiarrhythmic drug. Diazepam (**3**), also known as Valium, is a central nervous system depressant. Finally, fluoxetine hydrochloride (**4**) is a widely used antidepressant recognized by its trade names Prozac and Sarafem.

As shown in Figs. 3 to 5, the synthesis of each API utilizes simple starting materials and reagents readily available from commercial suppliers and highlighted advantages that flow chemistry offers relative to batch synthesis. Synthetic schemes were first developed in flow on a microliter scale before translating to the platform. The reactions leverage quick exposure at elevated temperatures (130° to 180°C) and pressures (~1.7 MPa) in controlled environments to enable faster reactions with low impurity profiles and reduce total synthesis times from hours to minutes. Reagents were in high concentrations, close to saturation, and in some cases even neat, which ensured high productivity while reducing waste and solvent amounts. This is in contrast to batch conditions that use lower concentrations, as solvents often also serve as a heat transfer medium. Moreover, in the flow system, reaction and purification occurred at the same time at different locations within the same uninterrupted reactor network. In batch, each of the operations would be physically and temporally disconnected and would have much larger time, space, and workforce requirements, hence drastically increasing the global footprint and decreasing the global output of a given process.

Assembly of the platform

The system consists of reconfigurable upstream and downstream units (Fig. 1) that, despite having many complex operations, can be managed easily by an individual user. This is unlike typical batch manufacturing, which requires many operators to oversee multiple large-scale reactors and tanks with volumes on the order of thousands of liters and the transport and formulation of the final API in a separate processing plant (*23*). As shown in Fig. 1A, the upstream unit houses reaction-based equipment for producing APIs (e.g., feeds, pumps, reactors, separators, and pressure regulators) and has a maximum power requirement of 1.5 kW, which is mainly consumed by heating the reactors and operating the pumps. The backside (in Fig. 1A), alternatively, represents the downstream unit (Fig. 1B) dedicated to purification and formulation of the drug product (e.g., tanks to precipitate the crude API from reaction mixtures, crystallizers, and filters) (Fig. 1D). Temperature, pressure, flow, and level sensors

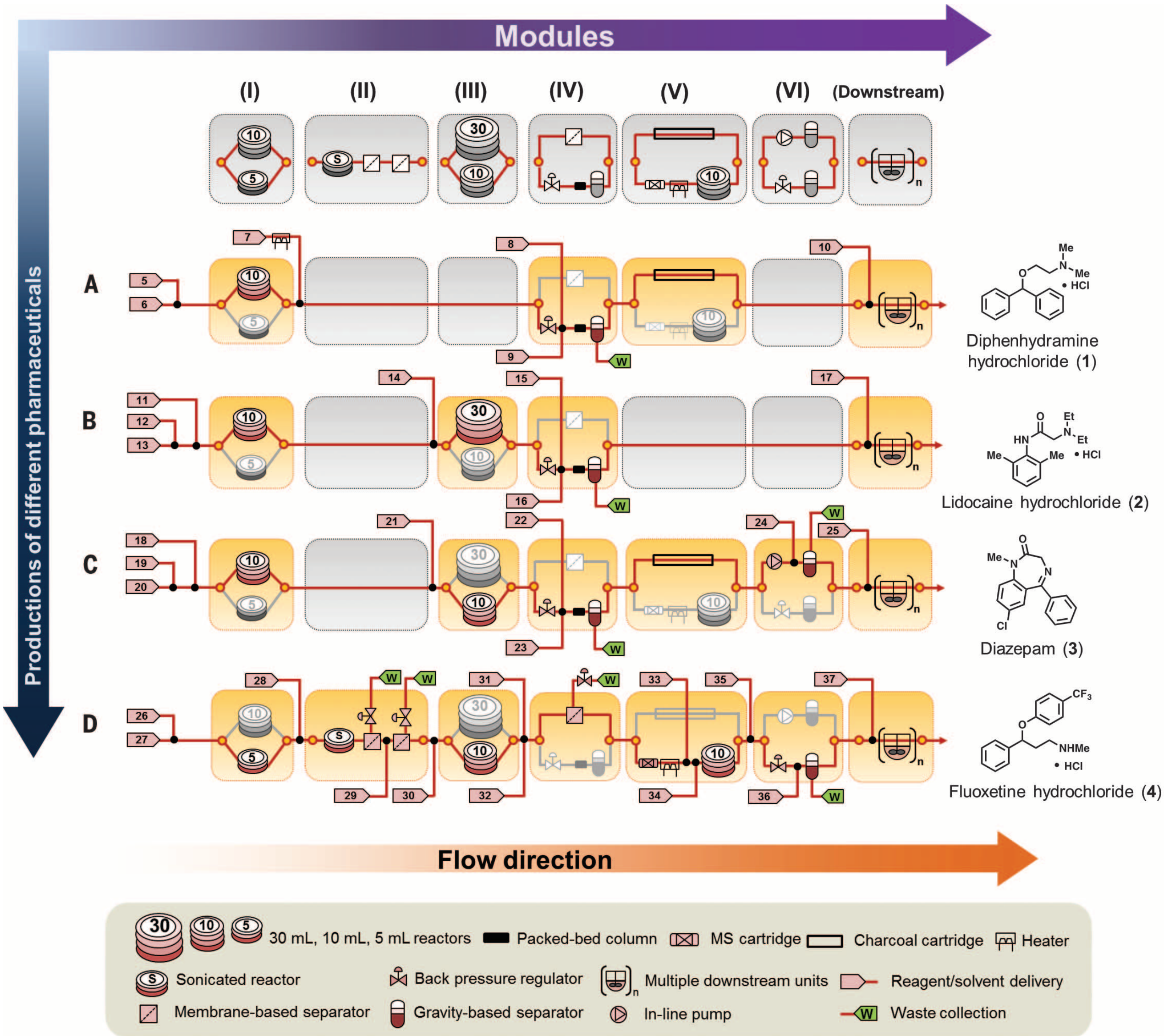

Fig. 2. Reconfigurable modules and flowcharts for API synthesis. (**A**) Diphenhydramine hydrochloride, (**B**) lidocaine hydrochloride, (**C**) diazepam, and (**D**) fluoxetine hydrochloride. The top row represents the different modules. Colored modules are active, gray boxes designate inactive modules. Reagent and solvent numbers refer to the compounds listed in table S2.

are included at strategic positions and coupled with data acquisition units to facilitate operational monitoring and support real-time production control. Because few commercial chemically compatible components were available and suitable for the gram-per-hour size scale combined with elevated temperatures and pressures, we developed most of the unit operations used in the upstream and downstream systems, as detailed in the supplementary text. These include pressure sensors, clamshell reactors with an outer aluminum body, and inner PFA (perfluoro alkoxy polymer) tubing for chemical compatibility with good heat transfer (Fig. 1C and fig. S5), surface tension liquid-liquid–driven extraction units (*24*) (Fig. 1C), multiline back pressure regulators (fig. S3), automated precipitation, filtration (Fig. 1D and fig. S6), and crystallization tanks, and automated formulation (Fig. 1D and figs. S7 and S8). The ventilation of this system was designed to have a face velocity between 0.4 and 0.5 m/s, which is typical for chemical fume hoods in the United States.

The units were arranged in modules of reactors and separators to enable reconfiguration to produce the four different drug products within the same system (Fig. 2; see table S2 for the numbering scheme). The synthesis schemes demonstrate the ability to reconfigure the system for increasing levels of chemical complexity, starting with diphenhydramine (Fig. 2A) with one reactor,

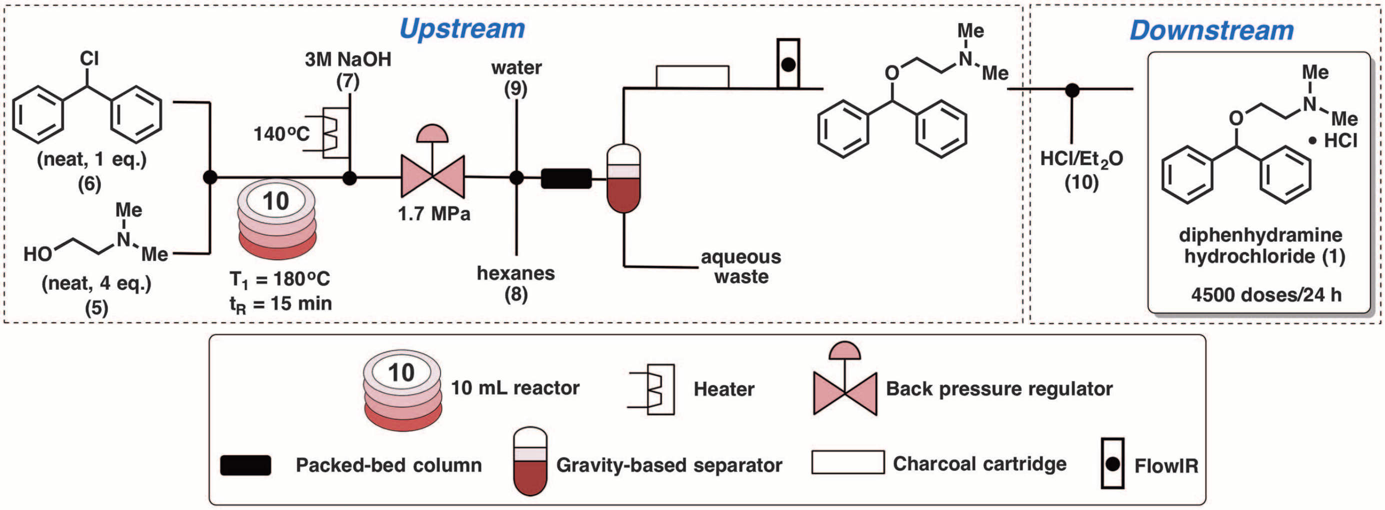

Fig. 3. Synthesis of diphenhydramine hydrochloride using the reconfigurable system. Flowchart detailing the upstream and downstream synthesis.

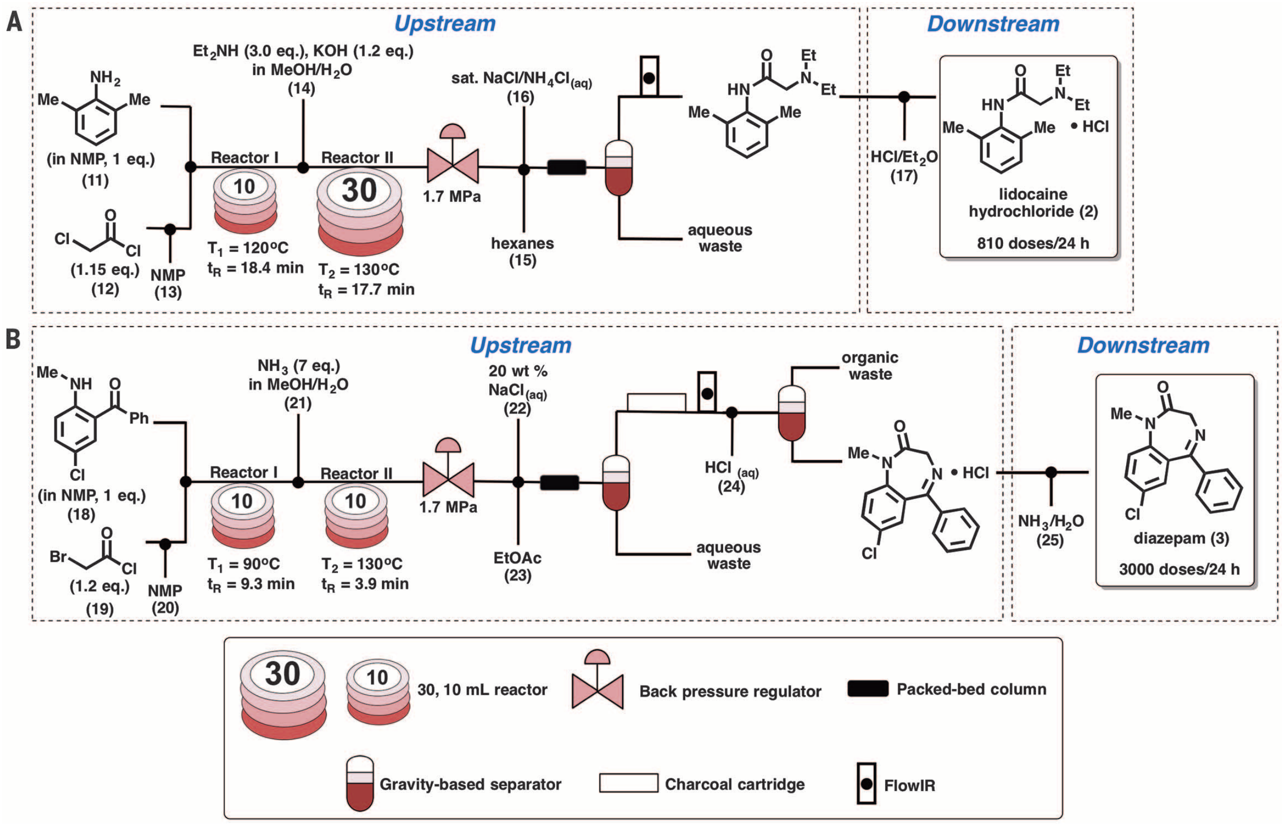

Fig. 4. Synthesis of APIs via two-step upstream configurations. (**A**) Lidocaine hydrochloride and (**B**) diazepam.

one separator, and four pumps and finishing with fluoxetine (Fig. 2D) with four reactors, four separators, and 11 pumps. An inline attenuated total reflection (ATR) Fourier transform infrared (FTIR) system (FlowIR) (figs. S9, S13, S14, S18, and S19) (*25*) provided real-time monitoring of the formed APIs. LabVIEW (National Instruments) programs were also implemented, along with the high- and fast-performance modular X Series data acquisition (DAQ) device and sensors for monitoring multiple process parameters—namely, pressure, reactor temperature, and flow rates. The same LabVIEW platform was also used to automate different units, including heating reactors, pumps, gravity-based separators, and multichannel valves. The downstream module alternatively (Fig. 2, right-hand modules) consisted of precipitation, filtration, redissolution, crystallization, filtration, and formulation units. All drug products were purified and formulated to meet U.S. Pharmacopeia (USP) standards. Consistent with the on-demand format, we focused on concentrated aqueous or alcohol-based formulations ready for dilution to target concentrations when needed and stable for at least 31 days (table S1). Solid formulations, such as tablets, would have required substantial additional space to house unit operations of drying, powder transport, solids blending, and tableting—all processes that would be difficult to implement on the gram-per-hour scale. Nevertheless, we are currently pursuing the miniaturization of these processes so that solid formulations may be prepared on the same platform.

Synthesis and formulation of diphenhydramine hydrochloride

As a first demonstration of the capabilities of this compact unit, diphenhydramine hydrochloride (**1**) was manufactured in its final liquid dosage form. As shown in Fig. 3, the process commenced with the reaction between an excess amount of neat 2-dimethylaminoethanol (**5**) and neat chlorodiphenylmethane (**6**) at a temperature of 180°C and a pressure of 1.7 MPa generated with the use of a back pressure regulator (BPR). The reaction was complete within 15 min, in contrast to typical batch processing requiring 5 or more hours at 125°C in benzene for a similar substrate (*26*). Because the product API has a melting point of 168°C, it could be handled in flow at 180°C in the absence of additional solvent, thereby minimizing the waste generated. The molten salt was then treated with a stream of preheated (140°C) aqueous NaOH (**7**). An inline purification and extraction process employing a packed-bed column to increase mass transfer, a gravity-operated liquid-liquid separator with automatic level control (fig. S1), and an activated charcoal filter to remove the colored impurities produced the diphenhydramine API as a solution in hexanes in 82% yield.

In the downstream section, the API was precipitated with HCl (**10**), and the resulting salt was filtered, washed, and dried in a specially constructed device with a Hastelloy filtration membrane (fig. S6) (*27*). After redissolving in isopropyl alcohol at 60°C, the diphenhydramine hydrochloride (**1**) was recrystallized in a crystallizer, while being cooled to 5°C. Upon filtering and drying, the crystals were dissolved in water. Real-time monitoring using an ultrasonic probe yielded the final dosage concentration (5 ml at 2.5 mg/ml). High-performance liquid chromatography analysis determined that the purity of the product conformed to USP standards (fig. S12) (*28*). Overall, the system capacity based on the optimal yield observed in each step was 4500 doses per day.

The facile transition from **1** to the production of lidocaine hydrochloride (**2**) (Fig. 4; see also Fig. 2B) was next accomplished through simple adjustments of the fluid manifolds to direct the fluids to specific reactors and separators. Whereas **1** was produced via a single upstream reaction, both **2** and **3** were generated through similar two-step upstream configurations, with modifications mainly in the purification and extraction regimens.

Synthesis and formulation of lidocaine hydrochloride

The synthesis of lidocaine hydrochloride (**2**) began with the acylation of 2,6-xylidine (**11**) in *N*-methyl-2-pyrrolidone (NMP) with neat chloroacetyl chloride (**12**), premixed inline with a stream of NMP (**13**) to avoid decomposition on standing (Fig. 4A; see also Fig. 2B). Subsequent addition of a stream of KOH and Et_2NH (**14**) in a mixture of polar protic solvents facilitated the installation of the tertiary amine to generate the crude API, without any intermediate purification. A BPR set at 1.7 MPa after reactor II enabled liquid flow at elevated temperatures (120°C and 130°C), allowing liquid operation well above the boiling point of diethylamine (55°C) and some of the solvents used (methanol and water). As a result, the reaction was complete within 5 min versus batch procedures of 60 min in refluxing toluene (*29*) or 4 to 5 hours in refluxing benzene (*30*). Overall, complete conversion (99%) of the starting materials to the crude API was realized in only 36 min. To deliver the crude lidocaine solution with sufficient purity for a streamlined downstream process, hexane (**15**) and a $NaCl/NH_4Cl$ saturated solution (**16**) were then injected through a cross-junction into the outlet product stream. Upon passing through a packed-bed column containing 0.1-mm glass beads and an inline gravity liquid-liquid separator, lidocaine was obtained in 90% yield. The downstream processing next proceeded with the formation of the HCl salt in a manner similar to that of diphenhydramine. After recrystallization, **2** (88% yield) had a purity of 97.7%, thereby meeting USP standards (fig. S17) (*31*). The API was treated with a premixed aqueous solution of 4% sodium methylcarboxycellulose to yield a final concentrate. Overall, this system can produce 810 doses (dosage strength = 20 mg/ml) of lidocaine hydrochloride per day.

Synthesis and formulation of diazepam

Following the production of lidocaine hydrochloride (**2**), we next transitioned to diazepam (**3**), through switching-in charcoal purification and gravity-based extraction units. As shown in Fig. 4B (see also Fig. 2C), the crude API was synthesized in a two-step upstream sequence initiated with the acylation of 5-chloro-2-(methylamino)

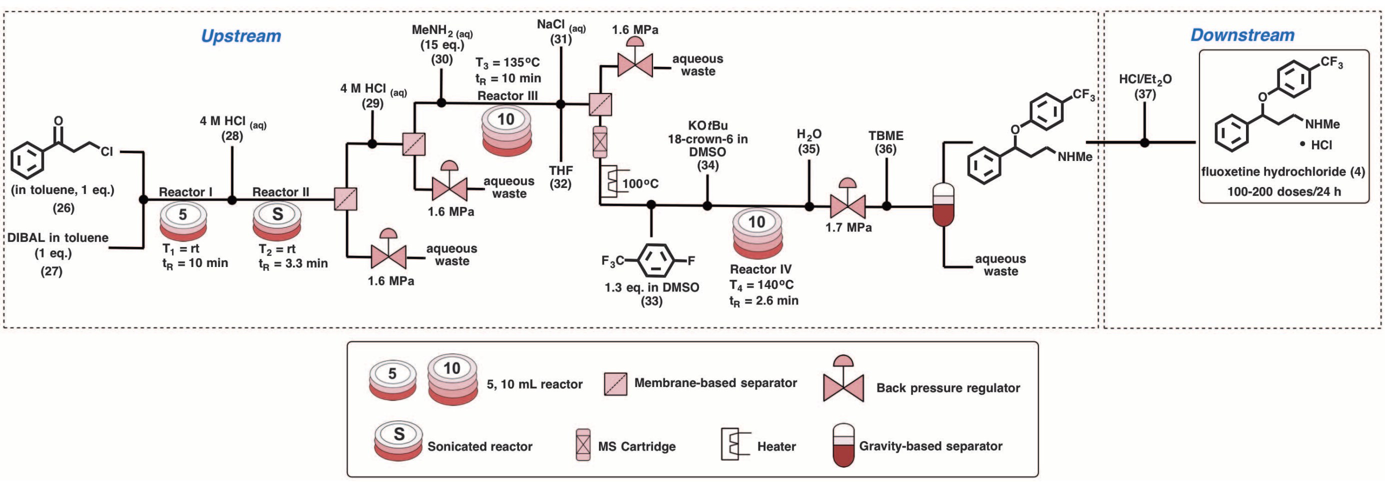

Fig. 5. Demonstration of a multistep API synthesis. Flowchart detailing the upstream and downstream synthesis of fluoxetine hydrochloride. DMSO, dimethyl sulfoxide; rt, room temperature; DIBAL, diisobutylaluminum hydride.

benzophenone in NMP (**18**) with neat bromoacetyl chloride (**19**) premixed inline with a stream of NMP (**20**). Bromine displacement, followed by an intramolecular cyclization reaction upon addition of a stream of NH_3 in $MeOH/H_2O$ (**21**), then furnished the target molecule. Similar to lidocaine, the application of elevated pressure (1.7 MPa) and temperatures (90°C and 130°C) in this sequence enabled liquid flow and complete conversion of the starting materials in only 13 min compared to 24 hours of batch operation at room temperature (*32*). After a continuous extraction, the organic stream was then passed through the activated charcoal cartridge to remove the dark colored dimer and trimer side-products. After precipitation and recrystallization in the downstream section, the dried diazepam crystals (**3**) (94% yield) had a purity level that met USP standards (fig. S22) (*33*). Resuspending in ethanol in the formulation tank then provided a concentrate. At a dosage concentration of 1 mg/ml (one dose is 5 ml at 1 mg/ml), this system can produce ~3000 doses per day.

Synthesis and formulation of fluoxetine hydrochloride

The last of the APIs produced, fluoxetine hydrochloride (**4**), was specifically chosen to demonstrate the versatility and capacity of this system to carry out a complex, fully integrated, telescoped, multistep, biphasic synthesis (Fig. 5; see also Fig. 2D). A series of individual reactions carried out in flow, with purification and isolation of each intermediate in batch, has been previously demonstrated (*34*). By integrating four reactors and four inline separation units, however, we realized the continuous end-to-end synthesis of this API as a racemic mixture. As shown in Fig. 5, the entire upstream reactor network was maintained at 1.7 MPa through the use of multichannel BPR located near the end of the upstream unit. The synthesis commenced with a DIBAL (**27**) reduction of a close-to-saturated solution of 3-chloropropiophenone in toluene (**26**) at room temperature in the first reactor. A stream of 4 M aqueous solution of HCl (**28**) was then introduced, and the resulting mixture was subjected to ultrasound in the second reactor to enable fast dissolution of the aluminum salts and ensure long-term and stable operation of the system (*35*). A two-stage inline extraction and separation sequence with in-house–constructed membrane liquid-liquid/gas separators removed the aqueous waste and gas (*24*). An additional stream of aqueous HCl (**29**) injected into the system before the second separation ensured a complete quench of the reaction.

The intermediate alcohol next reacted with aqueous methylamine (**30**) at 135°C in the third reactor in a biphasic flow. After a residence time of 10 min, tetrahydrofuran (THF) (**32**) and aqueous NaCl (20 mol %) (**31**) efficiently extracted the resulting amino alcohol into a suitable organic solvent (THF) for nucleophilic aromatic substitution in the fourth reactor. Upon separation of the aqueous and organic phase, the latter passed through a cartridge containing 0.4-nm molecular sieves to remove residual water. After a short residence time of 2.6 min in the fourth reactor, the fluoxetine solution merged with a stream of water to prevent the precipitation of the KF salt. Extraction and separation produced a solution of fluoxetine in *tert*-butyl methyl ether (TBME) (**36**) in 43% yield and at a production rate corresponding to 1100 doses per day (one dose is 5 ml at 4 mg/ml) prior to downstream processing. Similar to the other three APIs, the downstream processing involved a precipitation and recrystallization sequence to provide fluoxetine hydrochloride crystals that met USP standards (fig. S25) (*36*). Redissolution in water yielded the final concentrate in 100 to 200 doses.

Overall, the total cycle times for the production and formulation of the APIs varied from 12.2 hours in the case of lidocaine hydrochloride to 47.7 hours for fluoxetine hydrochloride (table S3). Whereas the upsteam syntheses required three residence times (total of 0.7 to 1.3 hours) of the sequential reactions to achieve steady state, the downstream processes took much longer and were mainly dominated by the precipitation step. Because the system featured valves, convenient feed swaps (from reagents to solvents) and fast cleaning procedures between each API production were achieved. Appropriate solvent combinations were added to the reactor lines to flush the up- and downstream units. At the shortest, switching the production of lidocaine hydrochloride to diazepam required a total of 15 min for a complete flush of the internal lines in the upstream section. A switchover from the simplest to the most complex synthesis (diphenhydramine hydrochloride to fluoxetine hydrochloride) would take 2 hours. No cross-contamination was detected from run to run, and the results were reproducible within a standard deviation of 0.6% (diphenhydramine hydrochloride) to 4.7% (fluoxetine hydrochloride) yield for each API production within a single run. The downstream purification and formulation units required no reconfiguration—only the aforementioned flushing. Thus, all transitions between production runs could be completed in less than 4 hours. To meet current good manufacturing practices, one could consider replacing the perfluorinated tubing and membranes in the reactors, BPRs, and separators. The units were designed to facilitate such a replacement.

Outlook

For over a decade, the FDA has been working to stimulate modernization of small-molecule manufacturing, which is largely based on batch manufacturing processes (*37*, *38*). The vision of the FDA's Pharmaceutical Quality for the 21st Century Initiative is to create a more robust and flexible pharmaceutical sector capable of manufacturing high-quality APIs. Continuous manufacturing is one such strategy for meeting this vision (*1*, *39*). Continuous manufacturing systems benefit from integrated processing and control, which can translate to increased safety (no manual handling) and shorter processing times. The use of highly adaptable smaller equipment, which implements real-time monitoring, may also lower production costs and improve product quality (*1*, *37*, *38*). The present implementation of four well-known pharmaceutical drugs demonstrates the concept of continuous, small-scale, on-demand production of pharmaceuticals. Already-demonstrated advances in flow chemistry (*11*–*20*) could be realized on similar platforms, and with additional research, ultimately enable the continuous synthesis of modern small-molecule pharmaceuticals, including enantiopure APIs. The current system focused on liquid oral and topical dosage formulations commensurate with the on-demand approach. A complete alternative platform to current batch manufacturing would inevitably have to produce pharmaceuticals in the common dosage forms of tablets and capsules as well as sterile injectable solutions, which would require advances in downstream processing. Specifically, classical unit operations of crystallization, drying, powder transport, solids blending, and tableting would have to be miniaturized and integrated. New approaches such as three-dimensional printing of tablets could facilitate these developments. Realization and demonstration of good manufacturing practices and ultimately FDA approval will be critical to future applications of this technology, including production units for hospitals, health care organizations, pharmaceutical development, and humanitarian aid.

REFERENCES AND NOTES

1. C. Badman, B. L. Trout, *J. Pharm. Sci.* **104**, 779–780 (2015).
2. I. R. Baxendale *et al.*, *J. Pharm. Sci.* **104**, 781–791 (2015).
3. S. Byrn *et al.*, *J. Pharm. Sci.* **104**, 792–802 (2015).
4. R. F. Service, *Science* **347**, 1190–1193 (2015).
5. S. Mascia *et al.*, *Angew. Chem. Int. Ed.* **52**, 12359–12363 (2013).
6. Food and Drug Administration, *Strategic Plan for Preventing and Mitigating Drug Shortages* (October 2013; www.fda.gov/downloads/Drugs/DrugSafety/DrugShortages/UCM372566.pdf).
7. L. Malet-Sanz, F. Susanne, *J. Med. Chem.* **55**, 4062–4098 (2012).
8. D. Webb, T. F. Jamison, *Chem. Sci.* **1**, 675–680 (2010).
9. R. L. Hartman, J. P. McMullen, K. F. Jensen, *Angew. Chem. Int. Ed.* **50**, 7502–7519 (2011).
10. V. Hessel, *Chem. Eng. Technol.* **32**, 1655–1681 (2009).
11. R. J. Ingham *et al.*, *Angew. Chem. Int. Ed.* **54**, 144–148 (2015).
12. B. Gutmann, D. Cantillo, C. O. Kappe, *Angew. Chem. Int. Ed.* **54**, 6688–6728 (2015).
13. M. Baumann, I. R. Baxendale, *Beilstein J. Org. Chem.* **11**, 1194–1219 (2015).
14. F. Lévesque, P. H. Seeberger, *Angew. Chem. Int. Ed.* **51**, 1706–1709 (2012).
15. M. D. Hopkin, I. R. Baxendale, S. V. Ley, *Org. Biomol. Chem.* **11**, 1822–1839 (2013).
16. C. A. Correia, K. Gilmore, D. T. McQuade, P. H. Seeberger, *Angew. Chem. Int. Ed.* **54**, 4945–4948 (2015).
17. M. Viviano, T. N. Glasnov, B. Reichart, G. Tekautz, C. O. Kappe, *Org. Process Res. Dev.* **15**, 858–870 (2011).
18. P. Zhang, M. G. Russell, T. F. Jamison, *Org. Process Res. Dev.* **18**, 1567–1570 (2014).
19. D. Ghislieri, K. Gilmore, P. H. Seeberger, *Angew. Chem. Int. Ed.* **54**, 678–682 (2015).
20. P. R. D. Murray *et al.*, *Org. Process Res. Dev.* **17**, 1192–1208 (2013).
21. P. L. Heider *et al.*, *Org. Process Res. Dev.* **18**, 402–409 (2014).
22. Materials and methods are available as supplementary materials on *Science* Online.
23. D. J. am Ende, in *Chemical Engineering in the Pharmaceutical Industry*, D. J. am Ende, Ed. (Wiley, NJ, 2011), chap. 1.
24. A. Adamo, P. L. Heider, N. Weeranoppanant, K. F. Jensen, *Ind. Eng. Chem. Res.* **52**, 10802–10808 (2013).
25. C. F. Carter *et al.*, *Org. Process Res. Dev.* **14**, 393–404 (2010).
26. G. Rieveschl, Dialkylaminoalkyl benzhydryl ethers and salts thereof, U.S. Patent 2,421,714A, 3 June 1947.

27. S. Y. Wong, J. Chen, L. E. Forte, A. S. Myerson, *Org. Process Res. Dev.* **17**, 684–692 (2013).
28. USP (U.S. Pharmacopeia), *Monograph* **34**, 2597 (2014).
29. T. J. Reilly, *J. Chem. Educ.* **76**, 1557 (1999).
30. N. M. Loefgren, B. J. Lundqvist, Alkyl glycinanilides, U.S. Patent 2,441,498, 11 May 1948.
31. USP (U.S. Pharmacopeia), *Monograph* **37**, 3552–3553 (2014).
32. T. Sugasawa, M. Adachi, T. Toyoda, K. Sasakura, *J. Heterocycl. Chem.* **16**, 445–448 (1979).
33. USP (U.S. Pharmacopeia), *Monograph* **37**, 2580–2581 (2014).
34. B. Ahmed-Omer, A. J. Sanderson, *Org. Biomol. Chem.* **9**, 3854–3862 (2011).
35. R. L. Hartman, J. R. Naber, N. Zaborenko, S. L. Buchwald, K. F. Jensen, *Org. Process Res. Dev.* **14**, 1347–1357 (2010).
36. USP (U.S. Pharmacopeia), *Monograph* **37**, 3035–3036 (2014).
37. Food and Drug Administration, *FDA Perspective on Continuous Manufacturing*, (February 2013; www.fda.gov/downloads/AboutFDA/CentersOffices/OfficeofMedicalProductsandTobacco/CDER/UCM341197.pdf).
38. S. L. Lee *et al*., *J. Pharm. Innov.* **10**, 191–199 (2015).
39. S. D. Schaber *et al*., *Ind. Eng. Chem. Res.* **50**, 10083–10092 (2011).

ACKNOWLEDGMENTS

Authors are listed in alphabetical order. We thank A. Clayton for elements of the system design, S. H. Harrison for the LabVIEW programming downstream, and A. T. Carlson for assistance with the design of the downstream units. We also thank L. M. Heckman and J. M. Noss for assistance with development of chemistry. This work was supported by the Defense Advanced Research Project Agency (DARPA) and Space and Naval Warfare Systems Center Pacific (SSC Pacific) under Contract no. N66001-l l-C-4147. We thank E. Choi, D. T. McQuade, J. Lewin, and G. Ling for their advice and support. The data reported in this paper are available in the article or in the supplementary materials. A.A. is founder of Zaiput Flow Technologies. T.F.J. is a cofounder of Snapdragon Chemistry, Inc., and a scientific adviser for Zaiput Flow Technologies, Continuus Pharmaceuticals, Paraza Pharmaceuticals, and Asymchem. K.F.J. is a scientific adviser for Snapdragon Chemistry, Inc. A.S.M. is a scientific adviser to GenSyn Technologies, Blues Spark Technologies, Continuus Pharmaceuticals, and Goddard Laboratories. MIT has filed a patent on behalf of A.A., M.B., T.F.J., K.F.J., J.C., A.S.M., J.-C.M.M., E.M.R., D.R.S., T.S., N.W., S.Y.W., and P.Z.

SUPPLEMENTARY MATERIALS

www.sciencemag.org/content/352/6281/61/suppl/DC1
Materials and Methods
Figs. S1 to S25
Tables S1 to S3
References (*40*–*43*)

21 December 2015; accepted 22 February 2016
10.1126/science.aaf1337

REPORTS

STELLAR EVOLUTION

A white dwarf with an oxygen atmosphere

S. O. Kepler,[1]* Detlev Koester,[2] Gustavo Ourique[1]

Stars born with masses below around 10 solar masses end their lives as white dwarf stars. Their atmospheres are dominated by the lightest elements because gravitational diffusion brings the lightest element to the surface. We report the discovery of a white dwarf with an atmosphere completely dominated by oxygen, SDSS J124043.01+671034.68. After oxygen, the next most abundant elements in its atmosphere are neon and magnesium, but these are lower by a factor of ≥25 by number. The fact that no hydrogen or helium are observed is surprising. Oxygen, neon, and magnesium are the products of carbon burning, which occurs in stars at the high-mass end of pre–white dwarf formation. This star, a possible oxygen-neon white dwarf, will provide a rare observational test of the evolutionary paths toward white dwarfs.

White dwarf stars are the end product of stellar evolution for all stars born with masses below 8 to 11 solar masses ($M_\odot$). The limit depends on the initial composition on the main sequence, in particular the abundances of the heavy elements (the metallicity), but also on uncertainties of the models and input physics. Among these are the nuclear reaction rates of C+He and C+C and the treatment of convection in the asymptotic giant branch (*1*, *2*). About 80% of white dwarfs have atmospheres dominated by H, and the remainder by He. All other elements are only small traces, much less abundant than in the Sun. The reason for this unusual pattern is separation in the strong gravitational field (*3*). The lightest elements present very rapidly float to the surface once the white dwarf cools below about 100,000 K effective temperature (T_{eff}). Except for the basic division of the two groups, which suggests different evolutionary channels, the atmosphere of the white dwarfs in their later cooling evolution has thus lost all memory of the previous evolutionary phases. There are only a few, very rare, exceptions to this rule. At very high effective temperature, T_{eff} > 200,000 K, two stars (H1504+65 and RX J0439.8-6809) (*4*) show no visible He or H but a C/O mixture. The limits on the He abundance are rather high, and it is quite possible that these stars will develop H or He atmospheres as they cool to lower effective temperatures, when gravitational separation becomes efficient.

Between 22,000 K ≥ T_{eff} ≥ 18,000 K, there is a small group of stars, called Hot DQ white dwarfs (*5*, *6*), which have C-dominated atmospheres. Their origin is not yet clear, but a likely scenario is that the carbon is dredged up from below the atmosphere once the convection zone reaches deep enough (*7*). If this scenario is correct, the DQ stars demonstrate that underneath the He layer there is a C layer resulting from the previous He-burning stage on the asymptotic giant branch. Another scenario is their formation by a merger of two white dwarf stars (*8*). At lower effective temperature, around 12,000 K, there is another small group of stars with strong O lines in their spectra; they have He-dominated atmospheres, but the next most abundant element is O, followed by C (*9*–*11*). It is plausible that their composition is related to the pre–white dwarf evolution, specifically C burning, but the reason that they appear at this temperature and this O/C ratio is not understood. To aid in our understanding of the late phases of low and intermediate mass star evolution, we searched for new white dwarf stars through the 4.5 million spectra in Data Release (DR) 12 (*12*) of the Sloan Digital Sky Survey (SDSS) (*13*).

One of the results of our search was SDSS J124043.01+671034.68 (spectrum with Plate-Modified Julian Date-Fiber 7120-56720-0894), which covers 3600 to 10,400 Å with resolving power $R = \lambda/\delta\lambda \sim 2000$. The spectrum (Fig. 1) exhibits many O I spectral lines, appearing similar to the group of cool stars with strong oxygen lines in their spectra (*10*, *11*). The absence of any He lines could be understood if the stellar effective temperature were near 11,000 K. However, closer inspection shows several lines of ionized Mg II and even O II, which require T_{eff} > 20,000 K. Temperatures ~20,000 K are also obtained from the SDSS photometry and the ultraviolet Galaxy Evolution Explorer (GALEX) measurements (*14*). At this temperature, the H and He lines, if these elements were present in the atmosphere, should be very strong. The absence of any He and H lines is only possible if O is the most abundant element. A detailed analysis (see the supplementary materials) confirmed this, with T_{eff} = 21,600 K and surface gravity log g = 7.93 ± 0.17, where $g = GM/R^2$ is the surface gravity in centimeter-gram-second units, with G the gravitational constant, M the stellar mass, and R the radius. Table 1 shows the atmospheric composition ratios determined from our modeling (see the supplementary materials).

The surface gravity is typical for white dwarfs (*13*) and corresponds to a mass of 0.56 ± 0.09 $M_\odot$, using the white dwarf mass-radius relation for stars without outer H layer (*15*), but it is theoretically not expected for a star with an oxygen atmosphere. From the estimated log g solution and the SDSS photometry in the *ugriz* filters,

[1]Instituto de Física, Universidade Federal do Rio Grande do Sul, 91501-900 Porto Alegre, RS, Brazil. [2]Institut für Theoretische Physik und Astrophysik, Universität Kiel, 24098 Kiel, Germany.
*Corresponding author. E-mail: kepler@if.ufrgs.br

Science
AAAS

On-demand continuous-flow production of pharmaceuticals in a compact, reconfigurable system

Andrea Adamo *et al.*

Science **352**, 61 (2016);
DOI: 10.1126/science.aaf1337